Joint Equalization and Multi-phase Tracking Based on MCC Criterion for Underwater Acoustic Communication

Miao Ke[1] and Zhiyong Liu[1,2,3](✉)

[1] Harbin Institute of Technology (Weihai), Weihai, China
lzyhit@hit.edu.cn

[2] Shandong Provincial Key Laboratory of Marine Electronic Information and Intelligent Unmanned Systems, Weihai 264209, China

[3] Key Laboratory of Cross-Domain Synergy and Comprehensive Support for Unmanned Marine Systems of Ministry of Industry and Information Technology, Weihai 264209, China

Abstract. In this paper, a multi-phase tracking (MT) structure based on decision feedback equalization is studied, which can solve the problem of strong multipath and phase offset in time varying underwater acoustic communication. Further, the joint equalization and multi-phase Tracking algorithm (JEMT) is proposed. The MT structure not only accelerates the convergence speed of phase tracking but also achieves better steady-state mean square error in equalization. In addition, considering that the noise in the actual underwater acoustic environment has obvious impulse noise characteristics rather than the Gaussian noise, this paper further proposes the JEMT algorithm based on the maximum correntropy criterion (JEMTMCC) to make it more suitable for the underwater acoustic environment. Finally, simulation results show that the JEMTMCC algorithm can achieve better bit error performance.

Keywords: Underwater Acoustic Time Varying Channel · Non-Gaussian Noise · Multi-Phase Tracking · Maximum Correntropy Criterion

1 Introduction

Underwater acoustic communication technology is the main way of long distance information transmission in the marine environment. However, compared with the environment of terrestrial wireless communication, the marine environment has the characteristics of strong multipath, time varying, and non-Gaussian noise, which leads to the degradation of communication quality.

Depending on the difference in transmission rate in underwater acoustic communication, the inter-symbol interference (ISI) caused by the multipath effect can span up to several tens of symbol intervals. To solve this problem, equalization is one of the commonly used research ways. However, perfect carrier recovery and symbol timing

H.-H. Chen and W. Meng (Eds.): WiSATS 2024, LNICST 605, pp. 226–236, 2025.
https://doi.org/10.1007/978-3-031-86196-3_19

are assumed in most research. The time varying ISI is the main reason for the bad capabilities of synchronization systems which are dominated by phase-locked loop (PLL) structure. In [1], phase parameter estimation and decision feedback equalization are jointly implemented to solve the problem of performance degradation caused by the interaction between equalization and phase estimation, and an adaptive algorithm combining phase estimation and equalization is designed. The second order PLL is used to estimate the phase parameters, the fractionally spaced decision feedback equalization (DFE) eliminates the need for symbol timing estimation, and the recursive least squares (RLS) algorithm with faster convergence speed improves the ability of fast-tracking. Subsequently, the authors extended this algorithm to spatial diversity and proposed an adaptive multichannel equalization and phase estimation algorithm [2]. Since the second order PLL and RLS algorithm increase a certain algorithm complexity compared with the conventional algorithm, some researchers consider the complexity of the system and algorithm and use different equalization algorithms (such as fast self-optimizing least mean square, FOLMS) and the structure of the first order PLL to study the joint phase estimation and equalization.

Another characteristic of the underwater acoustic environment is that underwater noise has obvious impulse noise characteristics, which do not conform to the nature of Gaussian distribution. Most equalization algorithms are based on the MSE standard and are carried out under the Gaussian assumption, which will lead to errors in the system performance when used in the actual system. To overcome this effect, some algorithms that can combat impulse noise, such as the affine projection algorithm and least mean M-estimation algorithm, have been introduced to deal with non-Gaussian noise [3, 4]. In recent years, an adaptive algorithm based on the maximum correntropy criterion (MCC) has been proposed to maximize the entropy between the desired signal and the output of the equalizer, which can effectively suppress impulse noise. After proving the mean square deviation (MSD) of the MCC in the adaptive filter, there have been several research directions on adaptive filtering algorithms for MCC. Kernel adaptive filtering [5, 6], convex merging optimization [7], and sparse adaptive filtering [8, 9].

As far as we know, the joint equalization and phase tracking algorithm based on MCC has not been studied yet, and the non-Gaussian noises in underwater acoustic communication cannot be ignored. Therefore, this paper will first study the joint equalization and single phase tracking algorithm based on MCC (JESTMCC). In addition, considering that the phase effect caused by the strong multipath effect in the underwater acoustic environment is the cumulative sum of the phase offset of multiple paths, and the single phase tracking structure cannot achieve the best phase compensation result, this paper plans to propose a multi-phase tracking (MT) structure to deal with the phase offset effect of multipath separately and combine this structure with MCC. To further improve the processing method for non-Gaussian and time varying multipath problems in underwater acoustic communication, the proposed joint equalization and multi-phase tracking algorithm based on MCC (JEMTMCC) will be verified by simulation.

The structure of this paper is as follows. Section 2 describes the time varying underwater acoustic multipath channel model and the adopted signal frame structure. In Sect. 3, We analyzed the channel model used in our research, the decision feedback equalization with the MT structure is introduced, and the JEMTMCC algorithm is described. The steady state error performance analysis is presented. In Sect. 4, the algorithm is simulated and compared with other algorithms. Finally, Sect. 5 summarizes the main conclusions of this paper as well as future research directions.

2 System Model

In this paper, the equalization algorithm of underwater acoustic communication receivers is mainly considered. In the whole system model, transmitted data bits are in turn passed through the modulation and waveform. The time varying channel and non-Gaussian noises will be considered. The simplified system model is shown in Fig. 1.

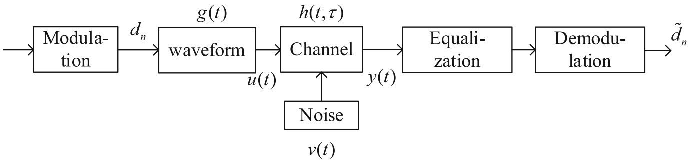

Fig. 1. System model

The purpose of the system design in Fig. 1 is that the original data bits can be recovered by the equalization algorithm at the receiver so that the probability $P(d_n \neq \tilde{d}_n)$ is minimized. Where d_n denotes the modulation symbol, $g(t)$ denotes the transmitted signal waveform, $u(t)$ denotes the baseband signal, $h(t, \tau)$ denotes the underwater acoustic channel model, $v(t)$ denotes the non-Gaussian noise, and $y(t)$ denotes the received signal.

In the modulation part, the carrier modulation part is ignored, and the modulated signal is expressed $\{+1, -1\}$ in the form of a constellation diagram. In this paper, QPSK modulation is used, and the baseband signal is specifically expressed as follows:

$$u(t) = \sum_n d_n g(t - nT) \tag{1}$$

where T denotes the symbol duration.

The underwater acoustic channel model is specifically expressed as formula (2).

$$h(t, \tau) = \sum_{p=1}^{L} A_P(t)\delta(\tau - \tau_p(t))e^{-j\varphi_p(t)} \tag{2}$$

where L denotes the number of multipath, $A_P(t)$ denotes the amplitude of the pth path, $\tau_p(t)$ denotes the delay of the pth path, $\varphi_p(t)$ denotes the phase offset of the pth path, and $\delta(\tau)$ is the unit impulse function.

The received signal can be expressed as follows.

$$y(t) = \sum_n \sum_{p=1}^{L} d_n A_P(t) g(\tau - nT - \tau_p(t))e^{-j\varphi_p(t)} + v(t) \tag{3}$$

The received signal is affected by channel fading, and the amplitude is generally small. Between equalization, we amplify the received signal by a certain proportion of power to avoid the situation that equalization is difficult to handle small values. In addition, the input method of equalization can be sampled with a symbol interval, but the best can be achieved only when the equalization length is infinite. In this paper, the fractional interval sampling method which is smaller than the symbol interval is used as the input signal of equalization, which can achieve better equalization performance.

The whole data frame can be divided into two parts. The first is the initial training phase, which may have multiple channel changes. The purpose is to make the equalization performance approach to the steady state, to facilitate the subsequent equalization and the tracking of the PLL. The second phase is the data phase, in which a small number of training sequences are used for supplementary training between each data packet, and the channel can be changed between any data packets.

3 Proposed Algorithm

3.1 Preprocessing

Firstly, this section will analyze the phase offset of the multipath channel. Under the condition of the underwater acoustic channel model described in Eq. (2), taking only two paths and the signal waveform represented by a rectangle as an example. When the phase offset of the first path is not affected by the phase offset of the following path, the phase compensation at the beginning of the second path has not eliminated the phase offset of the first path, so the PLL cannot achieve the desired effect.

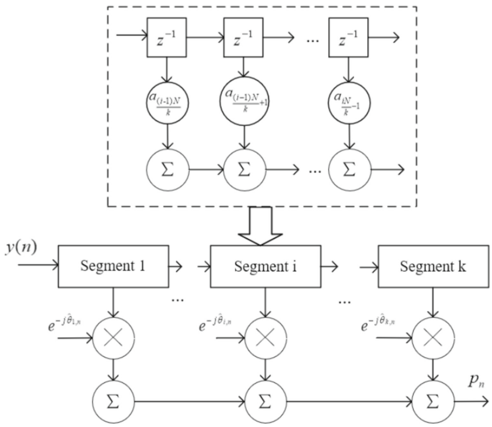

Fig. 2. MT Structure in Feedforward.

However, the inter-symbol interference is generally 20 ms above in the underwater acoustic channel, and the number of main paths of multipath is more than 5, which leads to the phase offset of more than one path when dealing with phase offset. Therefore, we further analyze and adjust the phase compensation in the specific equalization structure, and propose the MT structure, as shown in Fig. 2.

The input signal of equalization is generally obtained by sampling the received signal. In this paper, the received signal is sampled in the fractional interval mode, which is less than the symbol interval, and the sampling result of the received signal is represented. Then the output of feedforward equalization can be expressed as (4).

$$p_n = \sum_{i=0}^{N/k-1} y(n-i)e^{-j\widehat{\theta}_{1,n}}a_i + \cdots + \sum_{i=N/k}^{2N/k-1} y(n-i)e^{-j\widehat{\theta}_{2,n}}a_i + \cdots + \sum_{i=(k-1)N/k}^{N-1} y(n-i)e^{-j\widehat{\theta}_{2,n}}a_i = \sum_{l=1}^{k}(\sum_{i=(l-1)N/k}^{lN/k-1} y(n-i)a_i)\cdot e^{-j\widehat{\theta}_{l,n}} \tag{4}$$

Due to the existence of the segmented structure, the signal vector of the ith received signal at time n can be denoted as $\mathbf{y}_n[i] = [y(n-(i-1)N/k), \cdots, y(n-iN/k+1)]$, $\mathbf{a}_n[i] = [a_{(i-1)N/k}, \cdots, a_{iN/k-1}]$ denote the tap vector of the ith received signal at time n, N denotes the total length of the balanced taps, and k denotes the number of segments, which will be used in the following algorithm part. The above equation is further expressed in the form of vectors.

$$p_n = \mathbf{y}_n^T\Phi\mathbf{a}_n \tag{5}$$

where $\mathbf{\Phi} = diag[\underbrace{e^{-j\widehat{\theta}_{1,n}}}_{N/k}, \underbrace{e^{-j\widehat{\theta}_{2,n}}}_{N/k}, \cdots, \underbrace{e^{-j\widehat{\theta}_{k,n}}}_{N/k}]$ denotes the matrix consisting of phase offsets which is a diagonal matrix.

3.2 JEMTMCC Algorithm

This section introduces the JEMTMCC algorithm. MT structure is an improvement of the equalization structure. As decision feedback equalization is used in this paper, MT is mainly used in the feedforward part of the equalization, and the feedback part is consistent with the original equalization structure. The whole equalization structure will be shown in Fig. 3.

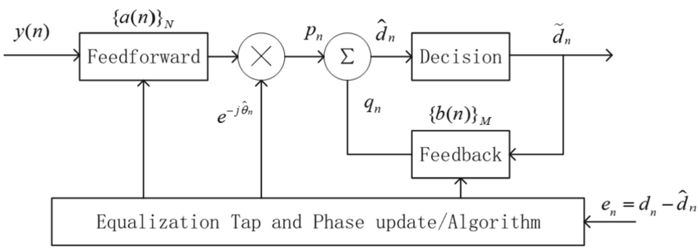

Fig. 3. Decision Feedback Equalization.

The input and tap of feedforward equalization and feedback equalization are represented by a vector.

$$\mathbf{w}_n = [\mathbf{a}_n, \mathbf{b}_n] \tag{6}$$

$$\mathbf{x}_n = [\mathbf{y}_n, -\widetilde{\mathbf{d}}_n] \tag{7}$$

The corresponding phase matrix is denoted as

$$\mathbf{\Phi} = diag[\underbrace{e^{-j\widehat{\theta}_{1,n}}}_{N/k}, \underbrace{e^{-j\widehat{\theta}_{2,n}}}_{N/k}, \cdots, \underbrace{e^{-j\widehat{\theta}_{k,n}}}_{N/k}, \underbrace{1}_{M}] \tag{8}$$

where M denotes the length of the feedback equalization. The error of equalization output can be expressed as follows.

$$e_n = d_n - \mathbf{w}_n^T \Phi \mathbf{x}_n \tag{9}$$

The optimization criterion of the JEMTMCC algorithm is maximization $\exp(-e_n^2/2\sigma^2)/\sqrt{2\pi}\sigma$, the corresponding partial derivatives are as follows

$$\partial/\partial \mathbf{w}_n = \exp(-e_n^2/2\sigma^2)\Phi \mathbf{x}_n e_n^*/\sqrt{2\pi}\sigma^3 \tag{10}$$

$$\partial/\partial\widehat{\theta}_{i,n} = -2\mathrm{Im}\{\exp(-e_n^2/2\sigma^2)/\sqrt{2\pi}\sigma^3 \cdot \mathbf{y}_n^T[i]\mathbf{a}_n[i] \cdot \mathrm{e}^{-j\widehat{\theta}_{i,n}})e_n^*\} \tag{11}$$

Table 1. The proposed JEMTMCC algorithm

Initialization	$\mathbf{a}_0[i] = \mathbf{0},\ \mathbf{b}_0[i] = \mathbf{0}$
Parameter	μ, η
	for n =1,2,3,... $\mathbf{y}_n[i] = [y(n-(i-1)N/k), \cdots, y(n-iN/k+1)]$ $\widetilde{\mathbf{d}}_n[i] = [\tilde{d}_{(i-1)N/k}, \cdots, \tilde{d}_{iN/k-1}]$ $\mathbf{x}_n = [\mathbf{y}_n, -\widetilde{\mathbf{d}}_n]$ $\mathbf{\Phi} = diag[\underbrace{e^{-j\widehat{\theta}_{1,n}}}_{N/k}, \underbrace{e^{-j\widehat{\theta}_{2,n}}}_{N/k}, \cdots, \underbrace{e^{-j\widehat{\theta}_{k,n}}}_{N/k}, \underbrace{1}_{M}]$ $e_n = d_n - \mathbf{w}_n^T \Phi \mathbf{x}_n$ $\mathbf{w}_{n+1} = \mathbf{w}_n + \mu \exp(-e_n^2/2\sigma^2)\Phi \mathbf{x}_n e_n^*/\sqrt{2\pi}\sigma^3$ $\widehat{\theta}_{i,n+1} = \widehat{\theta}_{i,n} - \eta \mathrm{Im}\{\exp(-e_n^2/2\sigma^2)/\sqrt{2\pi}\sigma^3 \cdot \mathbf{y}_n^T[i]\mathbf{a}_n[i] \cdot \mathrm{e}^{-j\widehat{\theta}_{i,n}})e_n^*\}$ *end*

3.3 Steady-State Mean Square Error Performance Analysis

The inputs of the feedforward filter and the feedback filter of the equalizer are combined, and the input of the feedforward part is multiplied by the phase compensation $\mathbf{x}_n$, which can be expressed as

$$\mathbf{x}_n = [\mathbf{a}_n e^{-j\hat{\theta}_n}, \mathbf{b}_n] \tag{12}$$

The error term in the tap coefficient update formula is represented by $f(e_n) = \exp(-e_n^2/2\sigma^2)e_n$, and the step size is denoted by $\eta = \mu/\sqrt{2\pi}\sigma^3$, , then (10–11) can obtain the following tap coefficient update formula

$$\mathbf{w}_{n+1} = \mathbf{w}_n + \eta f(e_n)\mathbf{x}_n \tag{13}$$

Assuming that the optimal tap coefficient is $\mathbf{w}_0$, after n times iterations the tap coefficient is $\mathbf{w}_n$, n times iterations the systematic error can be expressed as

$$e_n = (\mathbf{w}_0^T - \mathbf{w}_n^T)\mathbf{x}_n + v_n = \tilde{\mathbf{w}}_n^T \mathbf{x}_n + v_n = e_n^a + v_n \tag{14}$$

where e_n^a is the error of the equalization at the n iterations and v_n is the channel error.

Taking the expectation of Eq. (13), assuming that the input signal and channel noise are zero-mean and satisfy independent and identically distributed.

$$\begin{aligned} E[||\tilde{\mathbf{w}}_{n+1}||^2] &= E[||\tilde{\mathbf{w}}_n||^2] + \eta^2 E[f^2(e_n)||\mathbf{x}_n||^2] - 2\eta E[f(e_n)\tilde{\mathbf{w}}_n^T \mathbf{x}_n] \\ &= E[||\tilde{\mathbf{w}}_n||^2] + \eta^2 Tr(\mathbf{x})E[f^2(e_n)] - 2\eta E[f(e_n)e_n^a] \end{aligned} \tag{15}$$

When the number of iterations is sufficient, the equalizer can be regarded as having reached the steady state, and then the tap coefficient satisfies the following

$$\lim_{n\to\infty} E[||\tilde{\mathbf{w}}_{n+1}||^2] = \lim_{n\to\infty} E[||\tilde{\mathbf{w}}_n||^2] \tag{16}$$

$$2 \lim_{n\to\infty} E[f(e_n)e_n^a] = \eta Tr(\mathbf{x}) \lim_{n\to\infty} E[f^2(e_n)] \tag{17}$$

We simplified the left equation of Eq. (17), and let $E[||e_n^a||^2] = S$, (18) can be obtained.

$$\lim_{n\to\infty} E[f(e_n)e_n^a] = S \lim_{n\to\infty} E[f'(e_n)] \tag{18}$$

Using the expectation calculation formula, (18) can be simplified further.

$$f'(e_n) = (\exp(\frac{-e_n^2}{2\sigma^2})e_n)' = (1 - \frac{e_n^2}{\sigma^2})\exp(\frac{-e_n^2}{2\sigma^2}) \tag{19}$$

$$\lim_{n\to\infty} E[f'(e_n)] = \int_{-\infty}^{\infty} f(x)f_X(x)dx = \frac{1}{\sqrt{2\pi}\sigma_e}\int_{-\infty}^{\infty}(1 - \frac{e_n^2}{\sigma^2})\exp(-(\frac{\sigma^2 + \sigma_e^2}{2\sigma^2\sigma_e^2})e_n^2)de_n \tag{20}$$

Through a series of complicated integrals and simplifications.

$$\lim_{n\to\infty} E[f(e_n)e_n^a] = S\sigma^3/(\sigma^2 + S + \sigma_v^2)^{3/2} \tag{21}$$

$$\lim_{n\to\infty} E[f^2(e_n)] = \sigma^3(S + \sigma_v^2)/(2S + 2\sigma_v^2 + \sigma^2)^{3/2} \tag{22}$$

Substitute (21) and (22) into Eq. (17), lastly steady-state mean square error can be simplified as (23)

$$S = \frac{\eta\lambda Tr(\mathbf{x})\sigma_v^2}{2-\eta\lambda Tr(\mathbf{x})},\ \lambda = (\frac{\sigma^2+S+\sigma_v^2}{2S+2\sigma_v^2+\sigma^2})^{3/2} \tag{23}$$

When $\lambda = 1$ the steady-state error of the equalizer satisfying the JEMTMCC algorithm is equal to that of the LMS algorithm. Then $\lambda < 1$, we have

$$S_{JEST-MCC} < S_{LMS} = \frac{\eta Tr(\mathbf{x})\sigma_v^2}{2 - \eta Tr(\mathbf{x})} \tag{24}$$

4 Simulation Results and Analysis

4.1 Underwater Acoustic System Model Simulation

The statistical time varying underwater acoustic channel model proposed in [10] is used for the algorithm considered in this paper, while the symmetric α-stable ($S\alpha S$) model is used for the non-Gaussian noise model. The non-Gaussian noise waveform with symmetry parameter 0, offset parameter 1, and different characteristic parameters, represents the composition of large amplitude noise in non-Gaussian noise. The specific situation will be analyzed by simulation. In general, the range of values α in the $S\alpha S$ model is between 1 and 2.

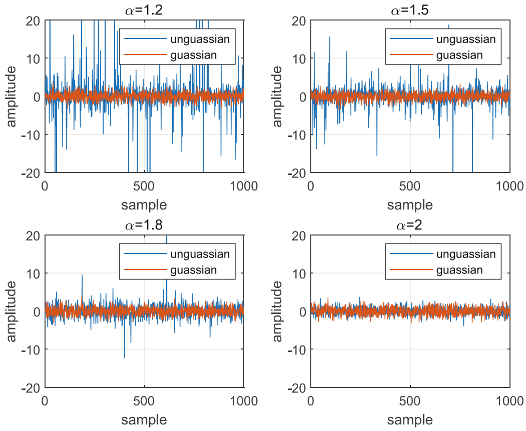

Fig. 4. Different α in $S\alpha S$ model

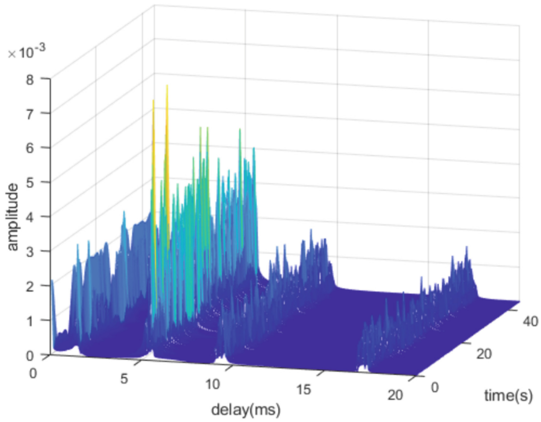

Fig. 5. Time varying underwater acoustic channel

Figure 4 in right above shows that when $\alpha = 2$, there is no large value amplitude noise, compared with Gaussian noise, which can be considered as Gaussian noise. With the decrease of α, when $\alpha = 1.8$, individual large amplitude noise appears; when $\alpha = 1.5$, the number of large amplitude noise increases; when $\alpha = 1.2$, larger amplitude noise appears, and the Gaussian component accounts for a small proportion. In the simulation, we adopt this model with $\alpha = 1.2$, 1.5, and 1.8 to simulate the non-Gaussian noise in the underwater acoustic communication algorithm test. Similarly, the underwater acoustic time varying model adopted in the simulation, as shown in Fig. 5. Multipath effect, which is mainly composed of five main paths, the arrival time of each main path will have a certain offset, and then the amplitude of different main paths will also change with time, which is in line with the characteristics of the underwater acoustic time varying channel.

4.2 Simulation of the Performance of the JEMTMCC Algorithm

The initial training consists of 1000 symbols, followed by symbols containing 1000 valid data to complete the information transmission process, and the simulation is repeated 300 times. The mixed signal-to-noise ratio (MSNR) is the ratio to the power of non-Gaussian noise Under this condition, the performance comparison between the JESTMCC algorithm and the JESTNLMS algorithm with different values is tested, and the results are shown in Fig. 6. In the models with different α, the BER performance of the two algorithms also becomes worse as the value decreases, which verifies that the large non-Gaussian value in the $S\alpha S$ model increases as the α decreases. In addition, the performance of the JESTMCC algorithm is slightly better than the JESTNLMS algorithm in the same model.

This result shows that the MCC algorithm achieves better BER performance than the MSE algorithm when the system noises are considered as non-Gaussian noise. We will consider the case of α 1.8 later in the validation of the algorithm.

In the same simulation environment, we continue to simulate and analyze the JEMTMCC algorithm proposed in this paper and the results are shown in Fig. 7.

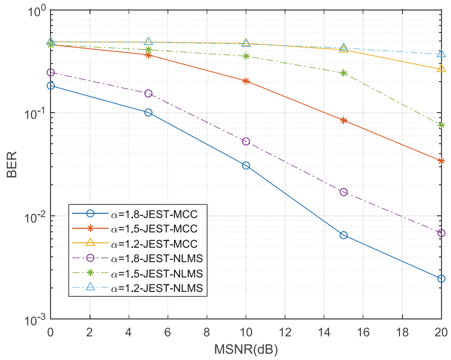

Fig. 6. Differences α in the JEST algorithm

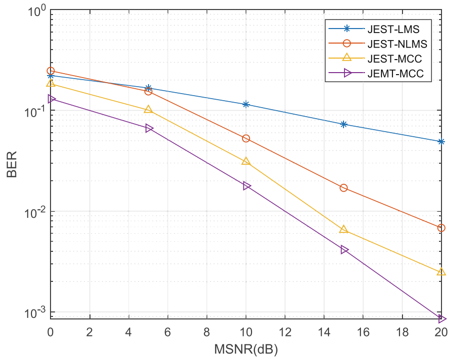

Fig. 7. BER performance of JEMT algorithms

From Fig. 7, we conclude that both JEMT and JEST algorithms fail to meet the desired system performance requirements at low SNR, and there is no significant difference in performance. However, compared with the MSE algorithm, the MCC algorithm still has a performance advantage. With the increase of SNR, JEMTMCC achieves an improvement compared to JESTMCC, which verifies the advantages of the MT structure proposed in this paper when facing time varying multipath channels.

5 Conclusion

In this paper, the non-Gaussian noise interference in time varying underwater acoustic communication systems is considered, and the multipath and phase offset problems in the actual channel are analyzed. An MT structure is proposed, and the JEMTMCC algorithm is proposed on this basis. The performance of the algorithm is tested under different non-Gaussian noise, different packet sizes, and different time varying factors. The results show that the JEMTMCC algorithm has the best robustness.

References

1. Stojanovic, M., Catipovic, J.A., Proakis, J.G.: Phase-coherent digital communications for underwater acoustic channels. IEEE J. Oceanic Eng. **19**(1), 100–111 (1994)
2. Stojanovic, M., Catipovic, J., Proakis, J.G.: Adaptive multichannel combining and equalization for underwater acoustic communications. J. Acoust. Soc. Am. **94**(3), 1621–1631 (1993)
3. Shao, T., Zheng, Y.R., Benesty, J.: An affine projection sign algorithm robust against impulsive interferences. IEEE Signal Process. Lett. **17**(4), 327–330 (2010)
4. Song, P., Zhao, H.: Affine-projection-like M-estimate adaptive filter for robust filtering in impulse noise. IEEE Trans. Circuits Syst. II Express Briefs **66**(12), 2087–2091 (2019)
5. Ma, W., Qu, H., Gui, G., Xu, L., Zhao, J., Chen, B.: Maximum correntropy criterion based sparse adaptive filtering algorithms for robust channel estimation under non-Gaussian environments. J. Franklin Inst. **352**(7), 2708–2727 (2015)
6. Chen, B., Xing, L., Liang, J., et al.: Steady-state mean-square error analysis for adaptive filtering under the maximum correntropy criterion. IEEE Signal Process. Lett. **21**(7), 880–884 (2014)
7. Chen, B., Xing, L., Zhao, H., et al.: Generalized correntropy for robust adaptive filtering. IEEE Trans. Signal Process. **64**(13), 3376–3387 (2016)
8. Shi, L., Lin, Y.: Convex combination of adaptive filters under the maximum correntropy criterion in impulsive interference. IEEE Signal Process. Lett. **21**(11), 1385–1388 (2014)
9. Li, Y., Jiang, Z., Shi, W., Han, X., Chen, B.: Blocked maximum correntropy criterion algorithm for cluster-sparse system identifications. IEEE Trans. Circuits Syst. II Express Briefs **66**(11), 1915–1919 (2019)
10. Wang, J., et al.: A novel underwater acoustic signal denoising algorithm for Gaussian/non-Gaussian impulsive noise. IEEE Trans. Veh. Technol. **70**(1), 429–445 (2020)